

## SYNTHESIS OF ZnO NANOPARTICLES AT DIFFERENT CONDITIONS: A COMPARISON OF PHOTOCATALYTIC ACTIVITY

MOHAMMAD A. BEHNAJADY\*, NASSER MODIRSHAHLA,  
ELNAZ GHAZALIAN

*Department of Chemistry, Faculty of Science, Islamic Azad University, Tabriz  
Branch, Tabriz, I. R. Iran*

Zinc Oxide (ZnO) nanoparticles have been synthesized by precipitation method using different precursors, under different conditions. ZnO nanoparticles were characterized by surface analytical methods such as x-ray diffraction (XRD), scanning electron microscope (SEM) and ultraviolet-visible spectroscopy. The XRD patterns of different ZnO nanoparticles suggest that the synthesized ZnO crystallites have hexagonal wurtzite structure. Variations in several parameters during synthesis process and their effects on crystallite size, morphology and photocatalytic activity of ZnO nanoparticles were investigated. The photocatalytic activity of ZnO nanoparticles was tested by photocatalytic removal of C.I. Acid Red 27 (AR27) as a model contaminant from monoazo textile dyes. Results show that photocatalytic activity of ZnO nanoparticles is very sensitive to precursors and synthesis process conditions.

(Received December 13, 2010; accepted February 22, 2011)

*Keywords:* C.I. Acid Red 27; Decolorization; heterogeneous photocatalysis; photocatalysis; zinc oxide nanoparticles

### 1. Introduction

Heterogeneous photocatalysis is a very promising method among advanced oxidation processes (AOPs), which can be conveniently applied for the degradation of pollutants [1-4]. In heterogeneous photocatalysis various semiconductors such as TiO<sub>2</sub>, ZnO, Fe<sub>2</sub>O<sub>3</sub>, CdS, and ZnS were used for removal of various contaminants [5]. Mechanism of heterogeneous photocatalysis includes reactions between adsorbed water, hydroxyl anions and oxygen molecules or other substances with electron-hole pairs produced at semiconductor surface under ultraviolet irradiation [1,2,5]. TiO<sub>2</sub> (Degussa P25) is extensively used as a standard active component for photocatalytic reactions [2,3]. The biggest advantage of ZnO in comparison to TiO<sub>2</sub> is that, it absorbs over a larger fraction of UV spectrum and the corresponding threshold of ZnO is 425 nm [1]. ZnO nanoparticles can be prepared by various methods such as alkaline precipitation, thermal decomposition, sol-gel technique and hydrothermal synthesis [6-9]. Daneshvar et al. [10] reported synthesis of ZnO nanoparticles from ZnSO<sub>4</sub>·7H<sub>2</sub>O as the starting material by precipitation method with high photocatalytic activity in the removal of diazinon as an insecticide. Kanade et al. [11] reported synthesis of ZnO nanoparticles with hexagonal wurtzite structure from zinc acetate as the starting material in aqueous and non-aqueous solvents and showed that ZnO nanoparticles prepared at aqueous media are more crystalline than samples prepared at non-aqueous media.

The aim of the presented work is to synthesize ZnO nanoparticles using different precursors under different conditions and to examine of its photocatalytic activity in the removal of C.I. Acid Red 27 (AR27) as a model contaminant from monoazo textile dyes. AR27 is used as a

---

\*Corresponding author: behnajady@gmail.com, behnajady@iaut.ac.ir

food dye, textile dye for wool and silk as well as in photography [12]. However, in 1970, Russian studies [13] showed that AR27 was carcinogenic.

## 2 Materials and methods

### 2.1 Materials

Zinc acetate [ $\text{Zn}(\text{CH}_3\text{COO})_2 \cdot 2\text{H}_2\text{O}$ ], zinc sulfate [ $\text{ZnSO}_4 \cdot 7\text{H}_2\text{O}$ ], oxalic acid [ $\text{H}_2\text{C}_2\text{O}_4 \cdot 2\text{H}_2\text{O}$ ], NaOH,  $\text{NH}_3$ , ethanol, poly-(ethylene glycol) with  $M_w$  4000 (PEG) and C.I. Acid Red 27 (AR27) were analytical grade and used as purchased. Solutions were prepared by dissolving appropriate amount of the compounds in double distilled water.

### 2.2 The synthesis of ZnO nanoparticles

#### 2.2.1 The first method

A certain amount of  $\text{ZnSO}_4 \cdot 7\text{H}_2\text{O}$  was dissolved in minimum amount of double distilled water, then NaOH or  $\text{NH}_3$  solution was added drop wise to the vigorously stirred above solution to adjust pH to about 7 until white precipitates were formed. Mechanical stirring or ultrasonic waves was used for stirring solution. The precipitates were filtered and washed with double distilled water. Then the wet powders were dried at about  $100^\circ\text{C}$  in an air oven. The dried solids were ground in an agate mortar and calcined at  $700^\circ\text{C}$  for 3 h [6].

#### 2.2.2 The second method

A certain amount of  $\text{Zn}(\text{CH}_3\text{COO})_2 \cdot 2\text{H}_2\text{O}$  was dissolved in 60 ml ethanol under vigorous stirring at  $60^\circ\text{C}$ . Then certain amount of  $\text{H}_2\text{C}_2\text{O}_4 \cdot 2\text{H}_2\text{O}$  was dissolved in 40 ml ethanol at  $50^\circ\text{C}$ . The oxalic acid solution under mechanical stirring or ultrasonic waves was added slowly to the warm ethanolic solution of zinc acetate. The formed white gel was dried at about  $100^\circ\text{C}$  in an air oven. The dried solids were ground in an agate mortar and calcined at  $500^\circ\text{C}$  for 3 h [14].

#### 2.2.3 The third method

A certain amount of  $\text{Zn}(\text{CH}_3\text{COO})_2 \cdot 2\text{H}_2\text{O}$  was dissolved in 60 ml ethanol under vigorous stirring at  $80^\circ\text{C}$ . Then certain amount of PEG was added into the above solution until all PEG was dissolved. Under ultrasonic waves, NaOH solution was added drop wise to adjust pH to about 7. The precipitates were filtered and washed with double distilled water. The wet precipitates were dried at about  $100^\circ\text{C}$  in an air oven. The dried solids were ground in an agate mortar and calcined at  $500^\circ\text{C}$  for 3 h [15].

### 2.3 The characterization of ZnO nanoparticles

The crystallite phase formation and size of ZnO nanoparticles were analyzed by X-ray diffraction (XRD) measurements which was carried out at room temperature, using Siemens X-ray diffraction D5000 with Cu  $K\alpha$  radiation ( $\lambda = 0.154056$  nm). The average particle size ( $D$  in nm) of ZnO nanoparticles was determined from XRD patterns of different ZnO samples according to the Scherrer's equation;

$$D = \frac{k\lambda}{\beta \cos \theta} \quad (1)$$

where  $k$  is a constant which equals to 0.89,  $\lambda$  is the X-ray wavelength which equals to 0.154056 nm,  $\beta$ , the full width at half maximum intensity (FWHM) and  $\theta$ , the half diffraction angle. Morphological characterization of ZnO nanoparticles was performed using SEM LEO 440i. Band gap of ZnO nanoparticles was determined from UV-Visible spectrum of ZnO nanoparticles dispersed in ethanol with ultrasonic waves by means of a double-beam UV-Visible spectrophotometer (Shimadzu 1700).

## 2.4 Photoreactor

Photocatalytic removal of AR27 with prepared ZnO nanoparticles was performed in a batch quartz tubular photoreactor of 100 mL volume with UV lamp (15 W, UV-C,  $\lambda_{\max} = 245$  nm, manufactured by Philips, Holland) in vertical array, which was placed in front of the quartz tube photoreactor [16].

## 2.5 Procedure

For the photocatalytic removal of AR27, a solution containing known concentration of the AR27 ( $20 \text{ mg L}^{-1}$ ) and ZnO nanoparticles ( $400 \text{ mg L}^{-1}$ ) was prepared and allowed to equilibrate for 30 min in the darkness. 100 mL of the prepared suspension was transferred into the reactor and then  $\text{O}_2$  was bubbled through the reactor with  $0.4 \text{ mL min}^{-1}$  flow rate. The reaction was initiated when the lamp was switched on and during irradiation,  $\text{O}_2$  flow was maintained in the photoreactor to keep the suspension homogeneous, then at certain reaction intervals, 5 mL of sample was withdrawn, centrifuged and the concentration of AR27 was determined by means of a UV-Vis spectrophotometer (Ultrospec 2000, Biotech pharamcia, England) at 522 nm. A calibration plot based on Beer-Lambert's law was established by relating the absorbance to the concentration.

## 3 Results and discussion

### 3.1 Photocatalytic activity of ZnO nanoparticles for the removal of AR27

Photocatalytic activity of ZnO nanoparticles prepared under different conditions with three methods was tested in the removal of AR27. The ZnO nanoparticles were synthesized with first method at different conditions such as stirring with ultrasonic waves or mechanical agitator and precipitation with NaOH or  $\text{NH}_3$ . Figure 1 shows semi-logarithmic graph of AR27 concentration versus irradiation time in the presence of ZnO nanoparticles synthesized with first method. Results in this figure show straight lines indicating pseudo first-order reaction. In all cases  $R^2$  (correlation coefficient) values were close to 0.99 which confirmed pseudo first-order kinetics for the removal of AR27 in this process.

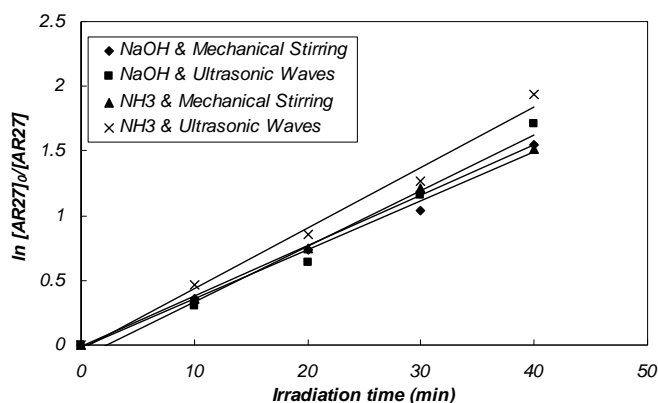


Fig. 1. Semi-logarithmic graph of AR27 concentration versus irradiation time in the presence of ZnO nanoparticles synthesized with first method at different conditions.

The photocatalytic oxidation kinetics of many organic compounds has often been modeled with the modified Langmuir-Hinshelwood equation [17-19] as Equation (2):

$$-\frac{d[AR27]}{dt} = \frac{k_{L-H} K_{ads} [AR27]}{1 + K_{ads} [AR27]_0} = k_{ap} [AR27] \quad (2)$$

which

$$k_{ap} = \frac{k_{L-H} K_{ads}}{1 + K_{ads} [AR27]_0} \quad (3)$$

where  $k_{L-H}$  the reaction rate constant ( $\text{mg L}^{-1} \text{min}^{-1}$ ),  $K_{ads}$  the adsorption coefficient of AR27 on the ZnO nanoparticles ( $\text{mg}^{-1} \text{L}$ ),  $t$  irradiation time (min),  $[AR27]$  the concentration of AR27 ( $\text{mg L}^{-1}$ ), and  $[AR27]_0$  is the initial concentration of AR27 ( $\text{mg L}^{-1}$ ). Equation (2) shows a pseudo-first order reaction with respect to the AR27 concentration. With integrating Equation (2) we obtain Equation (4) as following:

$$\ln \frac{[AR27]_0}{[AR27]} = k_{ap} t \quad (4)$$

According to Equation (4) apparent reaction rate constant ( $k_{ap}$ ) for the removal of AR27 in the presence of ZnO nanoparticles could be calculated from slope of straight lines in Figure 1 with linear regression analysis. The  $k_{ap}$  values obtained from Figure 1 were drawn in Figure 2 for different conditions. Results in this figure show ZnO nanoparticles prepared under ultrasonic waves and  $\text{NH}_3$  as precipitant agent have higher photocatalytic activity in the removal of AR27.

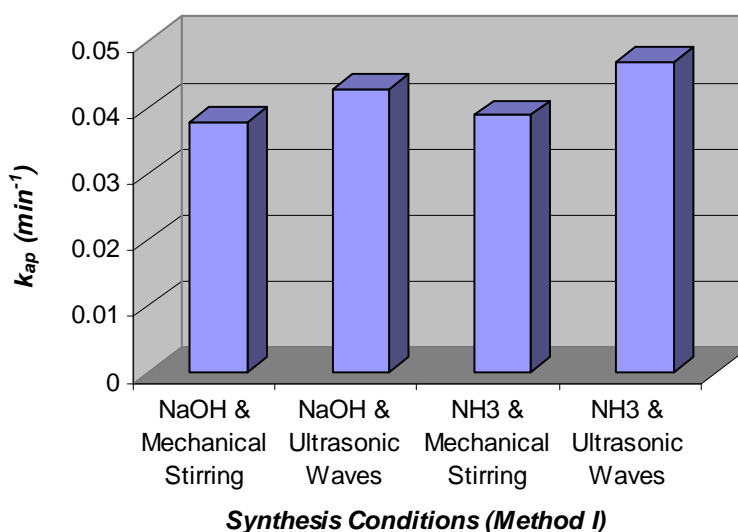


Fig. 2. The apparent reaction rate constant ( $k_{ap}$ ) for photocatalytic activity of ZnO nanoparticles synthesized with first method at different conditions.

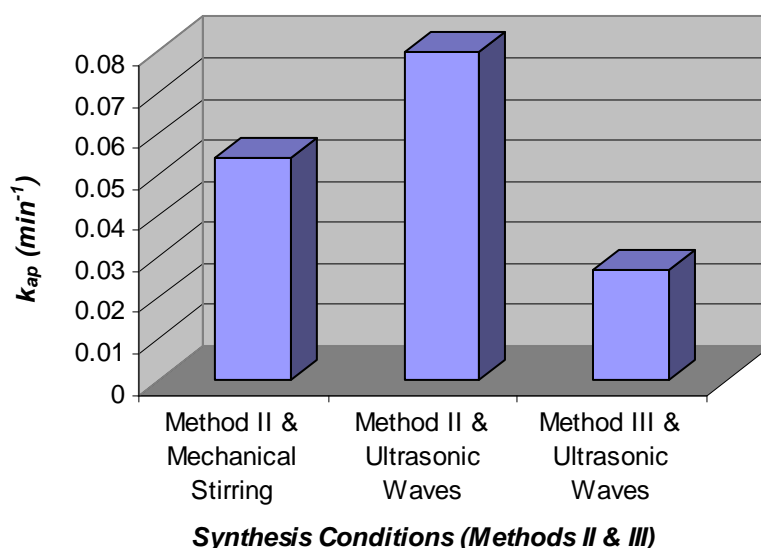


Fig 3. The apparent reaction rate constant ( $k_{ap}$ ) for photocatalytic activity of ZnO nanoparticles synthesized with second and third methods at different conditions.

ZnO nanoparticles were synthesized by second method at different stirring conditions with ultrasonic waves or mechanical agitator. The values of  $k_{ap}$  obtained for photocatalytic activity of ZnO nanoparticles prepared with second method at different conditions and also ZnO nanoparticles prepared with third method were reported in Fig. 3. Results in this figure and Figure 2, show ZnO nanoparticles prepared with second method under ultrasonic waves display higher photocatalytic activity in the removal of AR27. A comparison of  $k_{ap}$  values at Figure 2 and Figure 3 shows ZnO nanoparticles prepared with second method under ultrasonic waves and mechanical stirring show better photocatalytic activity than ZnO nanoparticles prepared with first and third methods. The order of photocatalytic activity of ZnO nanoparticles prepared at different conditions was as following:

Method II (Ultrasonic Waves) > Method II (Mechanical Stirring) > Method I (Ultrasonic Waves &  $\text{NH}_3$ ) > Method I (Ultrasonic Waves &  $\text{NaOH}$ ) > Method I (Mechanical Stirring &  $\text{NH}_3$ ) > Method I (Mechanical Stirring &  $\text{NaOH}$ ) > Method III (Ultrasonic Waves)

In third method PEG used as a capping agent which stabilize the ZnO nanoparticle [15], but the photocatalytic activity of ZnO nanoparticles was reduced considerably in the presence of capping agent.

### 3.2 The characterization of prepared ZnO nanoparticles

The XRD patterns of synthesized ZnO nanoparticles at different conditions were shown in Figure 4, for  $2\theta$  diffraction angles between  $5^\circ$  and  $70^\circ$ . The XRD pattern of ZnO shows nine primary peaks at  $31.8^\circ$ ,  $34.5^\circ$ ,  $36.3^\circ$ ,  $47.6^\circ$ ,  $56.8^\circ$ ,  $62.9^\circ$ ,  $66.4^\circ$ ,  $67.9^\circ$  and  $69.1^\circ$  which can be attributed to different diffraction ZnO planes. In the XRD patterns of synthesized ZnO nanoparticles especially with second and third methods, all peaks can be well indexed to the hexagonal wurtzite structure. ZnO nanoparticles synthesized with second and third methods are purer than nanoparticles synthesized with first method, because other peaks were observed in XRD pattern of ZnO nanoparticles synthesized with first method can be related to other phases of ZnO and impurities. The XRD pattern of second method shows wider peaks compared with the other two methods, which indicates its crystallites are ultrafine. The crystallite sizes calculated from

Scherrer's equation for ZnO nanoparticles synthesized with method II (Ultrasonic Waves), method I (Ultrasonic Waves & NH<sub>3</sub>) and method III (Ultrasonic Waves) were 14, 21 and 19, respectively.

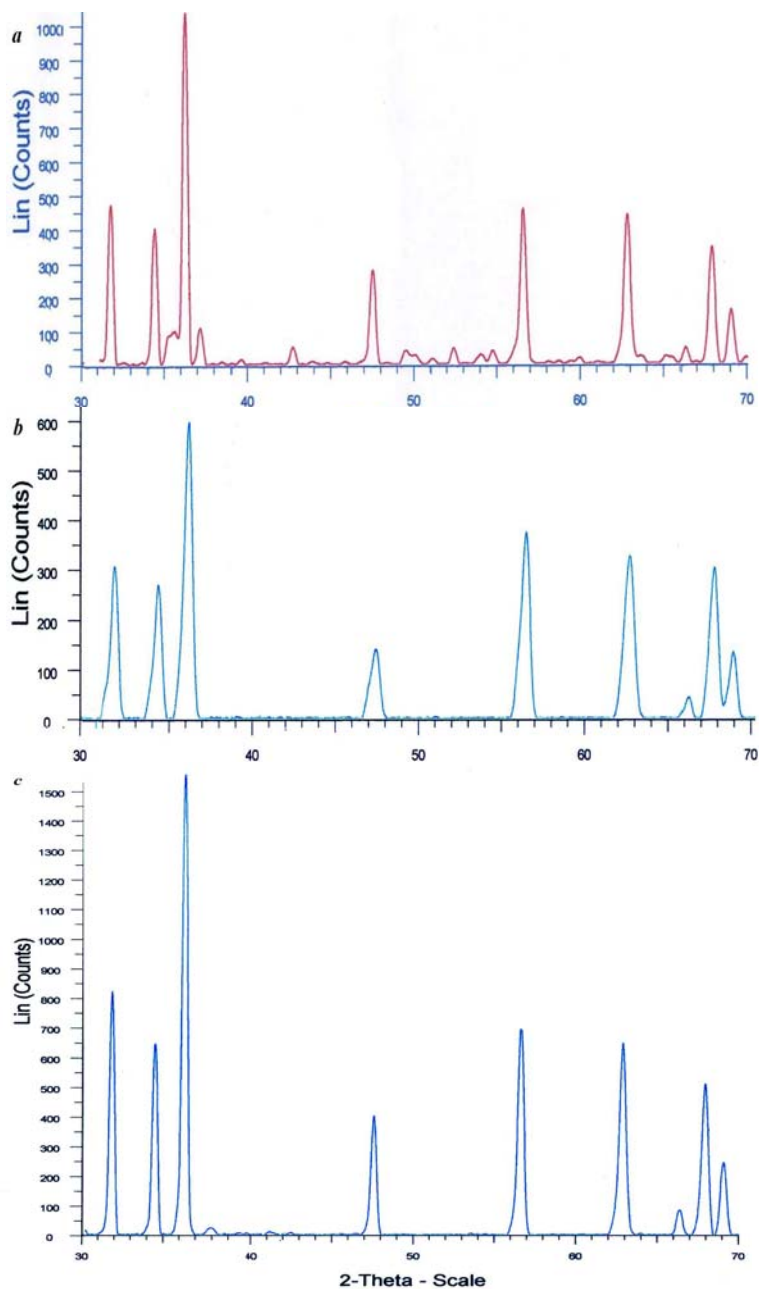


Fig. 4. The XRD patterns of ZnO nanoparticles: (a) first method; (b) second method and (c) third method

Figure 5 shows scanning electron micrographs (SEM) of ZnO nanoparticles synthesized with first and second methods. SEM pictures show more or less spherical particles at both methods, but agglomeration of particles was high in first method which can be resulted from high calcination temperature. ZnO nanoparticles synthesized with second method have a humdrum size distribution and small particles in comparison with first method.

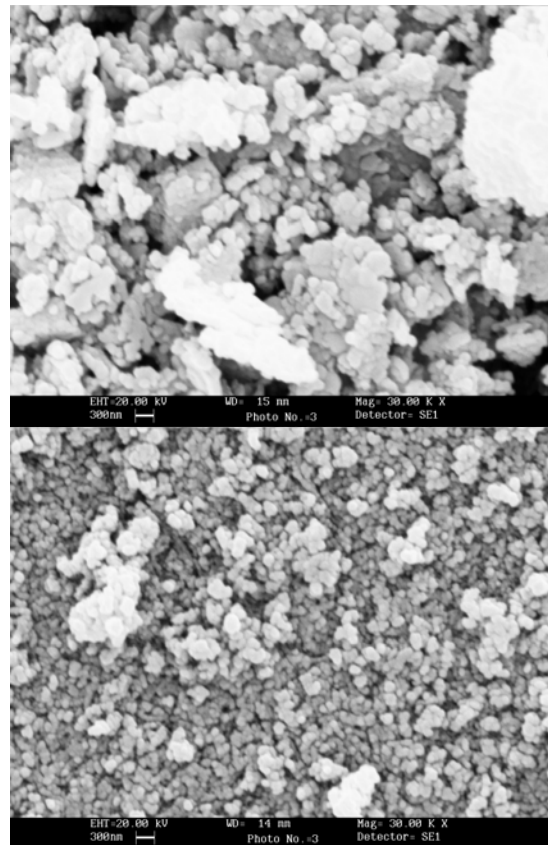


Fig. 5. SEM micrographs of ZnO nanoparticles: (top) first method and (bottom) second method

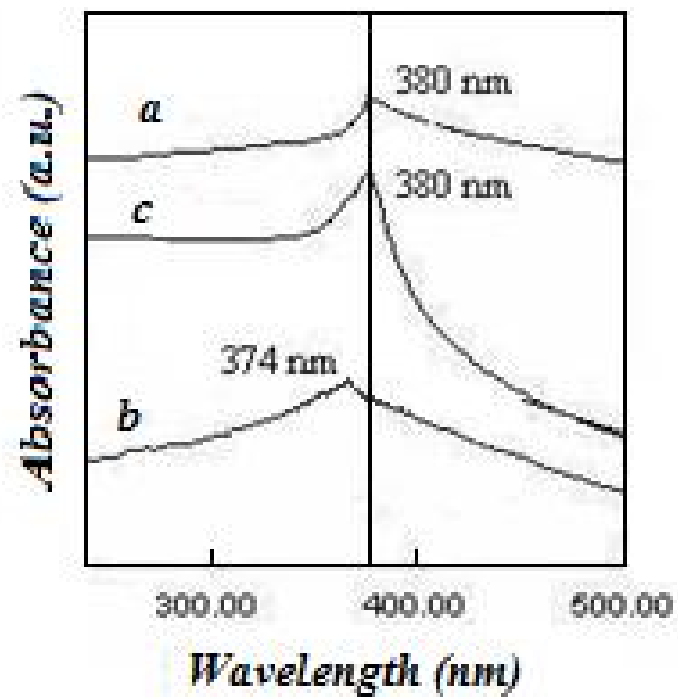


Fig. 6. UV-Visible spectrum of ZnO nanoparticles: (a) first method; (b) second method and (c) third method.

Figure 6 shows UV-Visible spectrum of synthesized ZnO nanoparticles dispersed in ethanol with ultrasonic waves. The absorption edge for ZnO nanoparticles synthesized with method II (Ultrasonic Waves), method I (Ultrasonic Waves & NH<sub>3</sub>) and method III (Ultrasonic Waves) were 374, 380 and 380 nm, respectively. These values correspond to band gaps 3.31, 3.26 and 3.26 eV. Blue shift was observed for ZnO nanoparticles synthesized with second method suggests a lower particle size. Smaller particle size and high band gap for ZnO nanoparticles synthesized with second method are important factors which can be effective at photocatalytic activity of ZnO nanoparticles.

#### 4. Conclusions

ZnO nanoparticles can be synthesized under different conditions. Ultrasonic waves can enhance photocatalytic activity of ZnO nanoparticles in the removal of AR27 as a model contaminant. ZnO nanoparticles synthesized from Zn(CH<sub>3</sub>COO)<sub>2</sub>·2H<sub>2</sub>O as a precursor, without addition of capping agent show high photocatalytic activity in the removal of AR27. ZnO nanoparticles, synthesized with this method have small particle size, humdrum size distribution and high band gap.

#### Acknowledgements

The authors thank the Islamic Azad University, Tabriz Branch for financial and other supports.

#### References

- [1] M.A. Behnajady, N. Modirshahla, R. Hamzavi, **133**, 226 (2006).
- [2] N. Daneshvar, M. Rabbani, N. Modirshahla, M.A. Behnajady, *J. Photochem. Photobiol. A* **168**, 39 (2004).
- [3] M.A. Behnajady, N. Modirshahla, N. Daneshvar, M. Rabbani, *Chem. Eng. J.* **127**, 167 (2007).
- [4] M.A. Behnajady, N. Modirshahla, N. Daneshvar, M. Rabbani, *J. Hazard. Mater.* **140**, 257 (2007).
- [5] O. Legrini, E. Oliveros, A.M. Braun, *Chem. Rev.* **93**, 671 (1993).
- [6] M. Zhang, T. An, X. Hu, C. Wang, G. Sheng, J. Fu, *Appl. Catal. A* **260**, 215 (2004).
- [7] C.-C. Lin, Y.-Y. Li, *Mater. Chem. Phys.* **113**, 334 (2009).
- [8] S. Rani, P. Suri, P.K. Shishodia, R.M. Mehra, *Sol. Energy Mater. Sol. Cells* **92**, 1639 (2008).
- [9] B. Baruwati, D.K. Kumar, S.V. Manorama, *Sens. Actuators B* **119**, 676 (2006).
- [10] N. Daneshvar, S. Aber, M.S. Seyed Dorraji, A.R. Khataee, M.H. Rasoulifard, *Sep. Purif. Technol.* **58**, 91 (2007).
- [11] K.G. Kanade, B.B. Kale, R.C. Aiyer, B.K. Das, *Mater. Res. Bull.* **41**, 590 (2006).
- [12] M. Karkmaz, E. Puzenat, C. Guillard, J.M. Herrmann, *Appl. Catal. B* **51**, 183 (2004).
- [13] M. Perez-Urquiza, J.L. Beltran, *J. Chromatogr. A* **898**, 271 (2000).
- [14] C. Hariharan, *Appl. Catal. A* **304**, 55 (2006).
- [15] Sh. Moradi, A. Madadi, presented at the 3<sup>rd</sup> Nanotechnology Students Congress, 2007, Iran.
- [16] M.A. Behnajady, N. Modirshahla, M. Shokri, H. Elham, A. Zeininezhad, *J. Environ. Sci. Health, A* **43**, 460 (2008).
- [17] C.S. Turchi, D.F. Ollis, *J. Catal.* **122**, 178 (1990).
- [18] H. Al-Ekabi, N. Serpone, *J. Phys. Chem.* **92**, 5726 (1988).
- [19] J. Beltran-Heredia, J. Torregrosa, J.R. Dominguez, J.A. Peres, *J. Hazard. Mater.* **83**, 255 (2001).